Anti-inflammatory and analgesic activities of the saponin, Daucosterol, and the triterpenoid ester, β-sitosterol 3-myristate, from *Capparis erythrocarpos*(Isert) Capparaceae, and their interaction with TRPV1 ion channel transporter

Emmanuel Kofi Kumatia

kofi2rhyme@yahoo.com

Centre for Plant Medicine Research, Mmpong-Akuapem. Ghana. https://orcid.org/0000-0002-7244-2751

Nguyen Huu Tung

Pheneeka University, Vietnam

Alex Asase

Centre for Plant Medicine Research, Mampong-Akuapem, Ghana.

Research Article

Keywords: Carrageenan, Transient receptor potential vanilloid 1 (TRPV1), Daucosterol, Saponin, Triterpenoid

Posted Date: May 6th, 2025

DOI: https://doi.org/10.21203/rs.3.rs-6232211/v1

Additional Declarations: The authors declare no competing interests.

Abstract

Capparis erythrocarpos root is an essential medicinal plant used in African traditional medicine as anti-arthritic, anti-inflammatory and analgesic agent. However, the chemical constituents in the plant responsible for its anti-inflammatory and analgesic activities were not known. This study reports on the isolation, characterization, anti-inflammatory and analgesic activities, of chemical constituents from the root bark of *C. erythrocarpos*. And also, determined the effect of these compounds on TRPV1 ion channels.

The isolated compounds which were characterized as Daucosterol (DC) and β-sitosterol 3- myristate (SM). DC significantly ($P < 0.05$) inhibited both phase 1 and phase 2 of carrageenan-induced edema inverse dose-dependently with anti- inflammatory activity of 58.38% at 2 mg/kg p.o. SM only inhibited the phase 2 of carrageenan-induced edema with anti-inflammatory activity ($P < 0.05$) of 22.57% at 2 mg/kg p.o. Furthermore, DC significantly ($P < 0.05$) inhibited the cold-induced and mechanical pains with analgesic activities of 257.30 ± 33.13% at 8 mg/kg p.o. and 47.37% at 2 mg/kg p.o. respectively. The analgesic activity calculated for SM under the same treatment was 201.80 ± 32.39% or 26.32% against cold-induced and inflammatory pains respectively. Diclofenac sodium (DC) 8 mg/kg p.o. (standard drug) produced significant ($P < 0.05$) anti-inflammatory activity of 53.07%, analgesic activity of 134 ± 19% against cold-induced pain and 42.11% against inflammatory pain respectively. DC and SM produced ΔG of -10.60 and 9.80 kcal/mol which were higher than 8.6 kcal/mol produced by DS in the molecular dynamic simulation studies. This indicates that the primary mode of action of DC and SM are through the TRPV1 ion channel whereas, DS have another mode of action apart from TRPV1 inhibition. These results indicates that Daucosterol and β-sitosterol 3-myristate possessed remarkable anti-inflammatory and analgesic activities. Daucosterol and β-sitosterol 3-myristate could therefore, be explored for the development of new analgesic and anti-inflammatory drugs.

1. Introduction

Pain is a vital sensation signaling tissue damage triggered by means of internal or external harmful occurrences (Sawynok, 2003). Inflammation of a wounded tissue or injury to the nerve in a damaged tissue, generates a booster input from nociceptive fibers to create a hyperexcitable conditions amongst nociceptive pathways in the CNS. This then leads to hyperalgesia, allodynia and impulsive pain (Price, 1996).

Cold temperature is one of the harmful stimuli which causes significant, irreparable tissue injury and painful sensation (Viana and Voets, 2019). Detection of cold or low temperatures therefore, is crucial for survival within the animal kingdom. Hence, various animals developed numerous approaches to lessen, circumvent and/or ran away from cold conditions (MacDonald et al., 2020).

The various classes of drugs, such as opioids, non-steroidal anti-inflammatory drugs (NSAIDs), anti-convulsants anti-depressant, and cannabinoids, presently available for the treatment of pain and inflammatory diseases produce severe adverse effects (Beal and Wallace, 2016; Bindu et al., 2020)

which in most cases, out weights their benefits. Hence, the need to develop novel potent analgesics which have less adverse effects.

Ion channels are widely distributed in tissues of vertebrates, with unlimited expression, and involvement in many biological processes in non-excitatory and excitatory cells. Transient Receptor Potential (TRP) ion channels are a family of non-selective cation channels which are characterized by 28 different members divided into six subfamilies including Transient Receptor Potential Vanilloids (TRPV) (Nilius and Owsianik, 2011). The TRPV subfamily is also made up of six members (TRPV1–6), of which TRPV1 channels are mainly located in neurons linked with pain perception, where they display extensive series of stimulative mechanisms, voltage dependance, selectivity, and pharmacological actions in contrast to any other ion channel clusters (Storozhuk, et al., 2019). These peculiar characteristics of the TRPV1 ion channels make them a target for the development of novel drugs for the treatment of pain, inflammatory diseases and cancer (Rahman et al., 2024; Bujak et al., 2019).

Capparis erythrocarpos, a medicinal plant found in the Capparaceae family, is a shrub which has abovate to elliptic or ovate and lanceolate shaped leaf with obtuse tip that curved at its base. The leaf which is 3–14 cm long and 1.5-5.0 cm in width has its surface shielded with clusters of small thorns (Kumatia et al., 2019; Mshana et al., 2000). The whole root or the root bark is the only part of the plant currently used for treatment in African traditional medicine. It is also the most widely studied part of the plant among its morphological organs. The root of *C. erythrocarpos* is prepared in different dosage forms to treat diseases such as, pain, inflammation, arthritis, blurred vision, and gas in the stomach (Mshana et al., 2000; Abbiw, 1990). Pharmacological activities reported of the plant are analgesic, anti-inflammatory, and anti-arthritic activities of the root; analgesic activity of thee stem; anti-malarial, anti-inflammatory and analgesic activities of the leaf (Kumatia et al., 2024; Kumatia et al., 2023; Kumatia et al., 2019).

So far, β-sitosterol, β-sitosterol myristate and β-sitosterol palmitate were isolate from the root bark of *C. erythrocarpos* and were shown to inhibit CFA-induced arthritis in rats (Kumatia et al., 2023). Betulinic acid was also isolated from the leaf and its anti-malarial activity elucidated (Kumatia et al., 2024). However, the anti-inflammatory activity of the chemical constituents of *C. erythrocarpos*' root against acute inflammation and pain are not known. The aim of this study therefore is to isolate, characterize the chemical constituents in the root bark of *C. erythrocarpos* and evaluate their anti- inflammatory and analgesic activities in laboratory rats.

2. Materials and methods

2.1. Chemicals

Analytical grades solvents such as petroleum ether (40–60 ^{o}C), chloroform and ethyl acetate were procured from Fisher Scientific (Loughborough, U.K) and Park Scientific Limited (Northampton, U.K.) respectively. Food grade ethanol (99%) was supplied by Midland Ghana limited (Tema). Silica gel (particle size 40–60 µm and 230 x 400 mesh size) and TLC plate (20 x 20 cm aluminum sheets

framework coated with TLC silica gel 60 F_{254}) were acquired from Sorbent Technologies (Atlanta, GA. USA) and Merck Chemicals (Damstadt, Germany) respectively. Diclofenac sodium (Research grade) was obtained from Sigma Chemical Co. (St. Louis, USA).

2.2. Collection, extraction and partitioning of C. erythrocarpos root bark

Collection, extraction and isolation of the compounds from the root bark of *C. erythrocarpos* was carried out using our previous methods (Kumatia et al., 2023a). *C. erythrocarpos* root was harvested in January 2017, from Dodowa, in the Shai Osudoku District of the Greater Accra Region of Ghana. The plant sample was assigned a voucher number CPMR 4876 and kept in the herbarium of CPMR (Kumatia et al., 2019). The root was cleaned with water and the bark removed, expurgated into fragments, dried in the sun for 10 days and milled. The course root bark powder (264.2 g) was extracted with 70% ethanol (2 x 625 mL) (EtOH) for 6 hours using the Soxhlet apparatus. The extraction process was repeated 12 times with 264.2 g each making the total quantity of the root bark extracted to be 3.17 kg. The ethanol was removed from the extract at 45 ^{o}C using the rotary evaporator. The resultant aqueous mixture was divided into 4 equal portions and successively partitioned with equal volumes of petroleum ether, PE, (0.663 L x 3) and ethyl acetate, EA, (0.663 L x 3). The PE or EA fraction was separately combined and dried with the rotary evaporator to obtain 10.28 g of CRPF (Capparis root petroleum ether fraction) and 6.78 g CREF (Capparis root ethyl acetate fraction) respectively.

2.3. Purification f petroleum ether fraction (CRPF)

Approximately, 10.28 g of CRPF mixed with silica gel and dried overnight. The mixture was transferred onto 225.00 g of normal-phase silica gel packed in a glass column and successively eluted with PE, PE-CF (chloroform) mixture with the CF being added at 5% until 100% CF was attained. CF – EtOH mixture was then applied with EtOH being added at 5% until 100% EtOH was attained. The individual fractions collected were combined separately into 6 groups (CRPF1 – CRPF6) using the similarities in their TLC profiles (Kumatia et al., 2023a).

CRPF3 (536.6 mg), an orange semi-solid, was further purified over 26.21 g wet silica gel in a small size glass column. The column was eluted with 100 mL each of the following solvent system: PE-CF 4/1; 7/3; 3/2; followed by CF-PE 1/1 (350 mL); CF 100% (200 mL); CF - EtOH 9/1 (200 mL). The fractions collected (68) were grouped into 3 (CRPF3 S1-S3) using their TLC profiles. CRPF3 S2, eluted with 100% CF, gave [1] (Kumatia et al., 2023a).

2.4. Purification of the ethyl acetate fraction (CREF)

CREF (6.78 g) was mixed with 23 g of silica gel and dried. Similar method was applied to purify dried sample as described above for the petroleum ether fraction CRPF to obtain CRPF1 -CRPF6. The fractions collected (150) were grouped into 5 major fractions CREF1-CREF6 (Kumatia et al., 2023a). Compound [2] was obtained from CREF4.

2.5. Development of TLC chromatograms of the compounds

The compounds were dissolved in chloroform and the solutions sported on a normal phase TLC plate on which the baseline and the solvent front was marked with parallel pencil lines. The plates were developed in the appropriate solvent system, stained with 10% H_2SO_4 and heated 80°C to develop the chromatograms.

2.6. NMR analysis of the compounds

Bruker FT-NMR Spectrometer (Avance TM 500 MHz, Germany) coupled with Bruker\TopSpin3.6.3, JJ 10 NMR data analysis software was employed to generate the NMR data (^1H, ^{13}C, ^1H-^1H COSY, DEPT135 and HMBC) of the compounds at room temperature. Tetramethylsilane was used as the internal standard and the chemical shift values given in δ (ppm). The compounds were dissolved in $CDCl_3$ and the solutions used for the analysis (Kumatia et al., 2023b).

2.7. Identification of carboxylic acid moieties

The carboxylic acid moiety of [1] was identified using the process of saponification and derivatization of carboxylic acids from the esters as described by Kumatia et al., (2023b). Briefly, around 2 mg of [1] was solubilized in methanol-sodium hydroxide solution (2 M) and heated for 1 h at 60 ℃ over water bath. The mixture was then taken of the water bath and 20 mL of distilled water added and cooled to room temperature. It was thereafter, extracted with 30 mL of n-hexane, the aqueous fraction acidified with 5 mL of 1 M HCl prior to its extraction with 20 mL of ethyl acetate. The ethyl acetate fraction was concentrated to 3 mL. About, 2 mL was poured into a GC vial and analyzed using GC-MS (Agilent 7890B) with Agilent GC Sampler 80 and Agilent 7000C Triple Quadrupole GC/MS) under the same conditions described in our previous study The carboxylic acid residue of [1] determined by assessment of its mass fragmentations and the search outcomes of the NIST mass spectra database (Kumatia et al., 2023b).

2.8. Pharmacological studies

2.8.1. Experimental animals and administration of test substances

The female Wistar rats (88–129 g) used for the study were housed in aluminum cages under controlled temperature and pressure and given distilled water and commercial palette chow *ad libitum*. The experiments were conducted according to institutional, national and international standards after obtaining ethical clearance from the Centre for Plant Medicine Institutional Review Committee. Administration of the compounds were conducted as follows: Groups 1–2 were given Daucosterol 2 and 8 mg/kg p.o. respectively. Groups 3–4 (2 and 8 mg/kg p.o.) of β-sitosterol myristate. Groups 5 and 6 were given Diclofenac sodium chloride powder (8 mg/kg p.o.), as standard control and 1 mL of distilled water as sham respectively.

2.8.2. Anti-inflammatory activity

The baseline paw widths (Lo) of the rats were measured using a digital caliper (Fisherbrand Traceable, Cat. No. 14-648-17, Fisher Scientific, China) prior to any treatment. Approximately, 10 min after the measurements, the various treatment agents were administered to the rats by oral gavage in 2% Tween 80 solution as vehicle. Thereafter, the inflammation was induced according to Winter et al., (1962) by sub-plantar of the right hind paw of each rat was injected with 0.2 mL of 1% carrageenan in normal saline. The paw width (Lt) of each rat was again measured at 1, 2, 3 and 4 h after the carrageenan injection. The anti-inflammatory activity of the compounds against carrageenan-induced paw edema was calculated as:

$$\mathrm{Ai} = \frac{\mathrm{Lt} - \mathrm{Lo}}{\mathrm{Lo}} \text{ x } 100\%$$

2.8.3. Evaluation of inflammatory pain using mechanical hyperalgesia test

On the 4th hour after induction of carrageenan-induced edema in the anti-inflammatory test above, the rats were restrained with the left hand and the right-hand fingers were used to gently press the inflamed paws 5 consecutive times. The number of vocalizations and / or withdrawal of the inflamed paw were recorded as pain. The analgesic activity (Aa) of each group was calculated with respect to the negative control using the formula:

$$\mathrm{Aa} = \frac{\text{Mean number of pain expressed by (treated group} - \text{control group)}}{\text{Mean number of pain expressed by control group}} \text{ x } 100\%$$

2.9. Cold pain test

The study was conducted by adopting the method of Zhao et al., (2013) with some modifications. Instead of the cold/plate, the rats were placed on cold ice blocks maintained at 1.50 ± 0.5 ℃. The reaction time (Tt) in seconds for paw licking, lifting, shaking or jumping was recorded. The baseline reaction time (To) was determined 1 h before administration of the drugs with the post drug administration reaction time determined at 1, 2, 3 and 4 h for each group. The analgesic activity (Aa) was calculated as:

$$\mathrm{Aa} = \frac{\mathrm{Tt} - \mathrm{To}}{\mathrm{To}} \text{ x } 100\%$$

2.10. Docking studies

Molecular dynamic stimulation studies of Daucosterol, β-sitosterol myristate and Diclofenac sodium were evaluated by employing cavity-detection guided blind docking approach with CB-Dock2 (Kumatia et

al., 2023c; Liu et al., 2022). The PDB arrangement of TRPV1 ion channel transporter protein 3j5p target protein was obtained from https://www.rcsb.org (RCSB PDB, 1971). Biova Discovery Studio 2023 (Dassault systems, 2023) was employed for visualization. Docking was initiated after water molecules and het atoms were removed from the protein.

3. Results

3.1. Characterization of the compounds

3.1.1. Structure identification of compound [1]

Compound **1** was obtained as orange solid (93.4 mg) which was soluble in chloroform. R_f = 0.6944 (Petroleum ether- ethyl acetate, 10:1). ^{1}H NMR ($CDCl_3$, 500 MHz), δ1.40 (2H, m, H-1), 1.5 (2H, m, H-2), 3.60 (1H, m, H-3), 5.48 (2H, m, H-4), 5.48 (1H, t, H-6), 2.05 (2H, m, H-7), 1.65 (1H, s, H-8), 1.6 (1H, s, H-9), 1.50 (2H, H-11), 1.5 (2H, m, H-12), 1.5 (1H, m, H-14), 1.60 (2H, m, H-15), 1.85 (2H, m, H-16), 1.50 (1H, m, H-17), 0.7 (2H, s, H-18), 1.00 (3H, s, H-19), 1.6 (1H, m, H-20), 0.90 (3H, d, H-21), 0.9 0.90 (2H, m, H-22), 0.90 (2H, m, H-23), 1.3 (1H, m, H-24), 1.6 (1H, m, H-25), 0.8 (3H, d, H-26), 0.90 (3H, d, H-27), 1.00 (2H, m, H-28), 0.80 (3H, t, H-29). 7.30 (1H, s, H-2'), 1.6 (1H, s, H-3'), 1.35 (1H, s, H-4'), 1.35 (1H, s, H-5'), 1.35 (1H, s, H-6'), 1.35 (1H, s, H-8'), 1.35 (1H, s, H-9'), 1.35 (1H, s, H-10'), 1.35 (1H, s, H-11'), 1.3 (1H, s, H-12'), 1.20 (1H, s, H-13'), 0.90 (1H, s, H-14'). ^{13}C NMR ($CDCl_3$, 500 MHz), δ 37.25 (C-1), 31.93 (C-2), 71.86 (C-3), 42.21 (C-4), 140.72 (C-5), 121.74 (C-6), 31.93(C-7), 31.93 (C-8), 50.15 (C-9), 36.51 (C-10),19.81 (C-11), 39.79 (C-12), 42.23 (C-13), 56.78 (C-14), 24.71 (C-15), 28.25 (C-16), 56.07 (C-17), 14.11 (C-18), 19.39(C-19), 36.15 (C-19), 36.15 (C-20), 18.78(C-21), 33.97 (C-22), 26.11 (C-23), 45.85(C-24), 29.70 (C-25), 19.81 (C-26), 19.04 (C-27), 23.08 (C-28), 14.11 (C-29), 179.0 (C-1'), 31.93 (C-2'), 29.70 (C-3'), 29.70 (C-4'), 29.70 (C-5'), 29.70 (C-6'), 29.70 (C-7'), 29.70 (C-8'), 29.70 (C-9'), 29.70 (C-10'), (C-11'), 24.71 C-12'), 22.69 (C-13'), 14.11 (C-14'). (Kumatia et al., 2023b).

3.1.2. GC-MS analysis of compounds [1]

The GC-MS spectra of the carboxylic acid moiety of **[1]** is shown in Fig 1. The RT of the carboxylic acid derivative of **[1]** was 12.91 minutes and was it was recognized in the NIST database to be tetradecanoic acid, also called myristic acid. The structure of **1** was confirmed as β-sitosterol 3-tetradecanoate (β-sitosterol 3-myristate) (Kumatia et al., 2023b).

3.1.3. Structure identification of compound [2]

Compound [**2]** was obtained as oyster white powder and gave positive Liebermann-Burchard reaction; the UV absorption was observed at 254 and 366 nm. The ^{1}H-NMR spectrum of **2** revealed the presence of an olefinic proton at δ_H 5.37 (1H, m, H-6), a hydroxymethin group at δ_H 3.60 (1H, m, H-3), 6 methyl groups, including 2 singlet signals at δ_H 0.71 (3H, s, H-18) and 1.03 (3H, s, H-19), 3 doublet signals at δ_H 0.94 (3H, d, J = 6.6 Hz, H-21), 0.83 (3H, d, J = 6.6 Hz, H-26), and 0.85 (3H, d, J = 6.6 Hz, H-27), and a triplet

signal at δ_H 0.86 (3H, t, *J* = 7.8 Hz, H-29), indicating that it had a sterol structure. Furthermore, the compound was found to have signals of the *β*-D-glucopyranose moiety with the presence of an anomeric proton [δ_H 4.40 (1H, d, *J* = 7.8 Hz, H-1')], a hydroxymethylene group [δ_H 3.76 (1H, dd, *J* = 5.4, 12.0 Hz, H-6') and 3.86 (1H, dd, *J* = 3.0, 12.0 Hz, H-6')], and four hydroxymethine groups [δ_H 3.20 (1H, m, H-2'), 3.38 (2H, m, H-3D, H-4D), and 3.27 (1H, m, H-5')], suggesting a sterol glycoside. In addition, the ^{13}C NMR spectrum of **[2]** revealed 35 carbon signals including two olefinic carbons at δ_C 140.4 (C-5) and 122.3 (C-6), one oxymethine at δ_C 79.3 (C-3), and an array of six carbons of a glucose unit [δ_C 101.2 (C-1D, Glc-1), 75.9 (C-2D, Glc-2), 77.3 (C-3D, Glc-3), 70.2 (C-4D, Glc-4), 77.7 (C-5D, Glc-5), and 61.9 (C-6D, Glc-6)], which were characteristic for stigmasterol glucoside. Furthermore, the ESI-MS showed a quasi-molecular ion peak at *m/z* 577.1 $[M + H]^+$ consistent with the molecular formula of $C_{35}H_{60}O_6$ (MW = 576). Based on the above evidence, the structure of **[2]** was identified as Daucosterol (**Fig. 2**).

Compound 2: R_f = 0.5952 (100% absolute ethanol); mp = 285-287^{o}C; [*α*] = -40 (c 0,5, CDCl3) ESI-MS: *m/z* 577.1 [M + H]+; ^{1}H-NMR (500 MHz, $CDCl_3$): δ_H 3.60 (1H, m, H-3), 5.37 (1H, m, H-6), 0.71 (3H, s, H-18), 1.03 (3H, s, H-19), 0.94 (3H, d, *J* = 6.6 Hz, H-21), 0.83 (3H, d, *J* = 6.6 Hz, H-26), 0.85 (3H, d, *J* = 6.6 Hz, H-27), 0.86 (3H, t, *J* = 7.8 Hz, H-29), Glc: 4.40 (1H, d, *J* = 7.8 Hz, H-1'), 3.38 (2H, m, H-3D, H-4D), 3.27 (1H, m, H-5'), 3.20 (1H, m, H-2'), 3.76 (1H, dd, *J* = 5.4, 12.0 Hz, H-6'), 3.86 (1H, dd, *J* = 3.0, 12.0 Hz, H-6'); ^{13}C NMR (125 MHz, $CDCl_3$): δ_C 37.4 (C-1), 28.4 (C-2), 79.3 (C-3), 42.5 (C-4), 140.4 (C-5), 122.3 (C-6), 32.0 (C-7), 31.9 (C-8), 50.3 (C-9), 36.8 (C-10), 21.1 (C-11), 38.8 (C-12), 42.5 (C-13), 56.9 (C-14), 24.4 (C-15), 28.4 (C-16), 56.2 (C-17), 11.9 (C-18), 19.4 (C-19), 36.3 (C-20), 18.9 (C-21), 34.1 (C-22), 26.2 (C-23), 46.0 (C-24), 29.3 (C-25), 19.9 (C-26), 19.1 (C-27), 23.2 (C-28), 12.0 (C-29), 101.2 (C-1D, Glc-1), 75.9 (C-2D, Glc-2), 77.3 (C-3D, Glc-3), 70.2 (C-4D, Glc-4), 77.7 (C-5D, Glc-5), 61.9 (C-6D, Glc-6).

3.4. Anti-inflammatory activity

The results of the effects of administration of Daucosterol (DC) and β-sitosterol 3-myristate (SM) on carrageenan-induced paw edema in rats are shown below in Fig. 3.

The inhibitory effect of Daucosterol (DC) 2 mg/kg p.o. on the Carrageenan-induced edema commenced from the first hour after its administration ($P < 0.05$) and got more pronounced through the second to the fourth hour ($P < 0.05$ to 0.0001) on the time course curve (Fig.3A). DC produced inverse dose-dependent inhibition of Carrageenan-induced edema in rats' paw. β-sitosterol 3-myristate (SM) also elicited an inverse dose-dependent inhibition of the Carrageenan-induced edema in rats' paw. However, the effect was statistically insignificant ($P > 0.05$) from the first to the fourth hour at both doses (Fig. 3C, D). On the other hand, the overall anti-inflammatory response shows that SM at 2 mg/kg p.o. was significant ($P < 0.05$). The anti-inflammatory effect of SM was less pronounced than that of Daucosterol. The anti-inflammatory activity produced by DC at 2 and 8 mg/kg p.o. on were 58.38 and 41.28% respectively. SM at 2 and 8 mg/kg p.o. also produced anti-inflammatory activity of 22.57 and 4.49 % respectively. The anti-inflammatory activity of the standard drug DC was 53.07%.

3.5. Analgesic activity of Daucosterol (DC) and β-sitosterol 3-myristate (SM)

3.5.1. Effect of Daucosterol (DC) and β-sitosterol 3-myristate (SM) on inflammatory pain

The effect of Daucosterol (DC) and β-sitosterol 3-myristate (SM) on inhibition of hyperalgesia instigated by Carrageenan-induced edema in rats' paws on the fourth hour is shown below in Fig. 4 A and B respectively.

DC and SM both inverse dose-dependently inhibited the mean reaction count of the rats. The effect was significant ($P < 0.05$) for DC at 2 and 8 mg/kg p.o. but statistically insignificant for SM at the same doses. The standard drug, DS, also produced significant ($P < 0.05$) inhibition of hyperalgesia in Carrageenan-induced edema with analgesic activity of 42.11%. (Fig. 4). Daucosterol (DC) at 2 and 8 mg/kg p.o. inhibited the Carrageenan-induced edema hyperalgesia with analgesic activity of 47.37 and 42.11% respectively. β-sitosterol myristate (SM) at 2 and 8 mg/kg p.o. also produced analgesic activity of 26.32 and 15.79% respectively.

3.5.2. Effect of Daucosterol (DC) and β-sitosterol 3-myristate (SM) on ice-induced cold pain

The effect of Daucosterol (DC) and β-sitosterol 3-myristate (SM) on cold-induced pain is shown below in Fig. 5 A-D. Both DS and SM significantly ($P < 0.05$) and dose-dependently protected the rats against cold-induced pain by increasing their latency to react to touch by cold ice.

The analgesic effect of DS at 8 mg/kg p.o., against cold-induced pain, commenced on the second hour after it was administered. The overall analgesic effect of DC was significant ($P < 0.05$) at both doses of 2 and 8 mg/kg p.o. with analgesic activity of 143.00 ± 27.55% and 257.30 ± 33.13% respectively. These values were significantly higher than 33.22 ± 7.99 % analgesic effect produced by the Negative control (2% Tween 80%) group. SM also, showed inverse dose-dependent analgesic effect with that of SM 2 mg/kg p.o. being significant ($P < 0.05$) compared to the negative control. The analgesic activity of SM 2 and 8 mg/kg p.o. were 201.80 ± 32.39% and 96.79 ± 27.00% respectively.

3.6. Molecular dynamic stimulation results

The results of the molecular dynamic stimulation between Daucosterol (DC), β-sitosterol 3-myristate (SM) or Diclofenac sodium (DS) is shown below in Table 1. DC crystal complex formed with TRPV1 produced the lowest ΔG of -10.60 kcal/mol compared to G of obtained for SM and DS. Furthermore, analysis of the various animo acids involved in the crystal structure formation of each compound with TRPV1 shows that SER 404 was present in the interaction of al the three compounds with TRPV1. However, the amino acid, TYR401was present only in the interaction of the two natural compounds isolated from *C. erythrocarpos*, which also produced the lowest ΔG compared to the standard synthetic drug, DS (Table 1).

4. Discussion

Carrageenan-induced paw edema model of inflammation is the most commonly used in vivo acute inflammation model employed to accessed the efficacy of anti-inflammatory agents. This model of inflammation was described as an extremely sensitive and reproducible assay used to evaluate nonsteroidal anti-inflammatory drugs (NSAIDs) and also employed to study novel anti-inflammatory agents (Willoughby and DiRosa, 1972). Carrageenan-induced paw edema assay is employed to predict the mechanism of action of orally active anti-inflammatory substances due to its phasic nature. The edema growth initiated with carrageenan injection into the rat's paw produces biphasic acute and local inflammatory response. The initial phase (which take place from 0–1 h) is controlled by the excessive biosynthesis of inflammatory mediators such as histamine, serotonin, and bradykinin. The final /second phase is governed by the synthesis of prostaglandins and different (pro or anti-inflammatory?) cytokines like TNF-α, IL-6, IL-10, and IL-1β (Crunkhorn and Meacock, 1971). The result of our study shows that Daucosterol (DC) administered orally at 2 mg/kg produced significant inhibition ($P < 0.05$) on the first hour and ($P < 0.05$) on the second to the fourth hour ($P < 0.0001$) on the Time-Course curve. This indicate that DC inhibited both the initial and the final stages of carrageenan-induced edema in rat paw. Therefore, the anti-inflammatory activity of the saponin, Daucosterol, involves the inhibition of histamine, serotonin, and bradykinin in the first phase in addition to PGs and pro inflammatory cytokines in the last phase.

β-sitosterol 3-myristate (SM) at 2 mg/kg p.o. also appears to inhibit the Carrageenan-induced edema in rats paw starting from the third hour although, the effect was statistically insignificant ($P > 0.05$) on the Time-Course curve due to the high standard error of mean (SEM). SM, however, did not produce inhibitory effect on the 0–2 hours after administration (Fig. 3C). This indicates that unlike DC which inhibited both phases of the carrageenan-induced inflammatory reaction, SM only inhibited the second phase and not the first phase. Suggesting that the mechanism of action of SM in acute inflammation involves the inhibition of PGs and proinflammatory cytokines, but does not inhibit histamine, serotonin, and bradykinins. Furthermore, the classical NSAID, Diclofenac sodium (DS) used as the standard drug also significantly ($P < 0.01$) only the second phase of the Carrageenan-induced edema but not the first phase (Fig. 3A and C), as expected. Since, DS is a standard COX-2 and COX-1 inhibitor.

The classical signs of inflammation are edema, erythema (redness), warmth, pain, and loss of function (stiffness and immobility). Carrageenan – induced edema in rat paw was reported to produce these classical signs of inflammation post subcutaneous injection (Morris, 2003).

Some cytokines are known to be involved in the instigation and argumentation of pathologic pain via activation of nociceptive sensory nerve cells. Certain pro-inflammatory cytokines such as IL-1β, IL-6, and TNF-α are also involved in nerve-injury/inflammation-induced central sensitization, and are related to the development of contralateral hyperalgesia (Zhang and An, 2007). Moreover, decreased in the production of pro-inflammatory cytokines was reported to reduce the severity of pain (Shavit et al., 2006). These theories suggest that anti-inflammatory substances which significantly inhibit the second phase of Carrageenan-induced inflammation will also demonstrate significant analgesic action against

inflammation-induced pain. Since the pro-inflammatory cytokines which initiate and sustain the pain are mostly produced during the second phase.

We therefore, set out to investigate if our isolated compounds can ameliorate the pain generated by the inflammation and the edema itself. The results shows that Daucosterol (DC) at 2 and 8 mg/kg p.o. produced significant ($P < 0.001$) inhibition of Carrageenan-induced inflammation hyperalgesia/pain with a maximum analgesic activity of 47.37% on the fourth hour. The analgesic activity of β-sitosterol 3-myristate (SM) 2 mg/kg p.o. and Diclofenac sodium powder (DS), in this model of pain, were 26.32% ($P > 0.05$) and 42.11% ($P < 0.01$) respectively. These results indicate that DC, SM and DS might inhibited the production of pro-inflammatory cytokines such IL-1β, IL-6, and TNF-α during the second phase of the inflammation to lessen the severity of pain.

It has been reported that transduction of cold stimuli is by direct stimulation of a cold-gated ion channel, blockade of the activity of voltage-gated Ca^{2+} ion channel, background K^{+} ion channel and / or inhibition of the Na+/K + ATPase (Foulkes and Wood, 2007).

Generally, there are two classes of thermoreceptors (Cold regulatory nociceptors) which regulate cooling effects in the mammalian body. They are low-threshold thermoreceptors which modulates mild cooling and high-threshold cold nociceptors which also modulates extreme cold (McDonald et al., 2020). C and A-delta low-threshold thermoreceptors are spontaneously active at neutral skin temperatures, but their firing frequency increases in response to small temperature drops, and rapidly adapts once steady-state temperature is reached. High-threshold cold thermoreceptors are generally dormant at normal and low body temperatures. However, they fire impulses in response to extreme cold in the noxious temperature region (McDonald et al., 2020).

Stimulation of TRPV1 initiates an influx of calcium and sodium ions, which leads to depolarization of cell membrane, firing by neurons, and release of endogenous substances, like substance P, bradykinin, calcitonin gene-related peptide, and glutamate, which modulate transmission of pain (Kort and Kym, 2012) and inflammation. Therefore, inhibition of TRPV1 channels leading to its deactivation produces analgesia and anti-inflammatory effect. It has been reported that a greater majority of TRPV1 antagonists, developed so far, block direct stimulation of nociceptors by endogenic lipids, capsaicin, acidic medium, and heat (Kort and Kym, 2012). The results obtained in the molecular stimulation studies shows that the Gibbs free energy (ΔG) of the crystal complex formed between TRPV1 and Daucosterol or β-sitosterol myristate or Diclofenac sodium were − 10.80, -9.80 and − 8.60 kcal/mol respectively. This indicates that these chemical entities also inhibit TRPV1 to produce analgesic and anti-inflammatory activities. It has also been reported that the higher the -ΔG value obtained for a docking result, the better the degree of inhibition (Gilson et al., 1997; Kumatia et al., 2023d). Therefore, Daucosterol or β-sitosterol myristate are better inhibitors of TRPV1 than Diclofenac sodium. This was confirmed in the animal studies where Daucosterol produced better anti-inflammatory and analgesic activities than β-sitosterol myristate and Diclofenac sodium. Moreover, although, β-sitosterol myristate show better inhibition of TRPV1 in the molecular stimulation studies ((ΔG = − 9.8 kcal/mmol), its analgesic and anti-inflammatory

effects were lower than that of Diclofenac sodium in the animal experiments. This shows that the primary mechanism of analgesic and anti-inflammatory action of Diclofenac sodium is through a different mechanism other than inhibition of TRPV1.

Daucosterol (DS) is a naturally occurring steroidal saponin which has glucose as the *glycone* bonded to C-3 of β-sitosterol, the aglycone. β-sitosterol myristate which is also a naturally occurring triterpenoid ester has myristic acid bonded to the C-3 of β-sitosterol as the alkanol group, instead of glucose in Daucosterol. Since, Daucosterol demonstrated better anti-inflammatory and analgesic activities than β-sitosterol myristate, indicates that substitution of a glucose/monosaccharide on C-3 of β-sitosterol leads to increased activity instead of substitution of carboxylic acid at the same position of β-sitosterol. This may be due to the presence of hyxdroxyl groups (4) in glucose which enhances easy dissolution and better bioavailability of Daucosterol compared to β-sitosterol myristate without any hydroxyl group.

Previous studies showed that Daucosterol possessed remarkable antioxidant and anti-inflammatory activities by inhibition of ROS, TNF-α, IL-1β, IL-6, IFN-γ and macrophage infiltration, hepatoprotective activity against alcohol-induced liver damage via the p38/NF-κB/NLRP3 pathway, and cardioprotective activity (Thanh et al., 2017, Jang et al., 2019; Zhang et al., 2023; Zhou et al., 2024). However, this is the first study to report the analgesic activity of Daucosterol against inflammation- and cold-induced pains and describe its isolation from *C. erythrocarpos*. Although, the anti-arthritic activity of β-sitosterol myristate and its isolation from *C. erythrocarpos* were previously reported (Kumatia et al, 2023a), this is first study to report on the acute anti-inflammatory and analgesic activities of β-sitosterol myristate, compare these activities with those of Daucosterol, and to also determine their influence on TRPV1.

5. Conclusion

This study has described the isolation and characterization of the steroidal saponin, Daucosterol, from *C. erythrocarpos* for the first time. It also shows that Daucosterol, possessed significantly high anti-inflammatory action and analgesic action, higher than those of Diclofenac sodium, against mechanical and cold-induced pain. β-sitosterol myristate. β-sitosterol myristate on the other hand, produced moderate anti-inflammatory and analgesic activities at the same doses as Daucosterol. Both compounds also, remarkably inhibited the TRPV1 ion channel with very low ΔG. Daucosterol and β-sitosterol myristate should therefore, be considered for development into potential analgesic and anti-inflammatory drugs.

Declarations

Data availability

Data available on request from the corresponding author.

Conflict of interest

The authors declare that they have no conflict of interest in this study.

Funding

This study received no specific funding.

Acknowledgement

The authors wish to express their gratitude to the staff of the Phytochemistry Department and Animal Experimentation Unit of Centre for Plant Medicine Research, Mampong-Akuapem, Ghana, for their technical support.

References

1. Sawynok, J. 2003. Topical and peripherally acting analgesics. Pharmacol Rev. 2003 Mar;55(1):1-20.
2. Price, D.D., 1996. Selective activation of A-delta and C nociceptive afferents by different parameters of nociceptive heat stimulation: a tool for analysis of central mechanisms of pain. Pain 68, 1–3.
3. Donald Iain MacDonald *,1, John N. Wood, Edward C. Emery. Molecular mechanisms of cold pain. Neurobiology of Pain 7 (2020) 100044. 1 – 11.
4. Viana, F, Voets, T, 2019. Heat pain and cold pain. In: J.N. Wood (Ed.), The Oxford Handbook of the Neurobiology of Pain, Oxford University Press 2019.
5. Beal, B. R. Wallac, M. S. 2016. An overview of pharmacologic management of chronic pain, Med. Clin. 100 (1), 65–79.
6. Bindu, S., Mazumder, S., Bandyopadhyay, U. 2014. Non-steroidal anti-inflammatory drugs (NSAIDs) and organ damage: a current perspective, Biochem Pharmacol.180, 114147.
7. Nilius B, Owsianik G. The transient receptor potential family of ion channels. Genome Biol. (2011) 12:218.
8. Storozhuk, MV, Moroz, O.F., Zholos, A.V. Multifunctional TRPV1 ion channels in physiology and pathology with focus on the brain, vasculature, and some visceral systems. Biomed Res Int, 2019 (2019), Article 5806321
9. Rahman, MM, Jo, Y.-Y, Kim, YH, Park C-K. 2024. Current insights and therapeutic strategies for targeting TRPV1 in neuropathic pain management. Life Sciences 355 (2024) 122954. 1-13.
10. Bujak, JK., Kosmala, D., Szopa, IM., Majchrzak, K, Bednarczyk, P. Inflammation, Cancer and Immunity —Implication of TRPV1 Channel. Front. Oncol. 9:1087.

11. Kumatia, E.K., Antwi, S., Brew-Daniels, H., Appiah, A.A., Ocloo, A. 2019. In vivo comparative anti-inflammatory and analgesic activities of root bark, stem and leaf extracts of Capparis erythrocarpus (Capparaceae). Pharmacognosy Journal. 11 (3), 515 - 520.

12. Mshana, N.R., Abbiw, D.K., Addae-Mensah, I., Adjanouhoun, E., Ahyi, M.R.A., Ekpere, J.A., Enow-Orock, E.G., Gbile, Z.O., Noamesi, G.K., Odei, M.A., Odunlami, H., Oteng-Yeboah, A.A., Sarpong, K., Sofowora, A., Tackie, A.N., 2000. Traditional Medicine and Pharmacopoeia: Contribution to the Revision of Ethnobotanical and Floristic Studies in Ghana. Organization of Africa Unity/ Scientific, Technical and Research Commission (OAU/STRC).

13. Abbiw, D.K. Useful plants of Ghana. 1st ed. Intermediate Technology Publications and Royal Botanic Gardens. London, Kew. 1990.

14. Kumatia, EK, Tung, NH, Asase, A. *Capparis erythrocarpos* (Isert) leaf and its principal constituent betulinic acid, elicit anti-malarial activity via immunomodulatory action and alleviation of thrombocytopenia in mice. Researchgate, 2024.

15. Kumatia, EK, Ocloo, A., Tung, N.H. 2023b. Triterpenoid esters from *Capparis erythrocarpos* (Isert), Capparaceae, root bark ameliorates CFA-induced arthritis. SaudiPharmaceutical Journal. 31 (2023), 698-705.

16. Kumatia, EK, Zoiku, F, Asase, A, Tung NH. Anti-malarial activity of the alkaloid, heptaphyline, and the furanocoumarin, imperatorin, from *Clausena anisata* against human *Plasmodium falciparum* malaria: *Ex-vivo* trophozoiticidal, schizonticidal and gametocytocidal approach. Malaria Journal. 22:264. https://doi.org/10.1186/s12936-023-04678-0.

17. Winter, C.A., Risely, E.A., Nuss, G.W., 1962. Carrageenan induced edema in hind paw of the rat as an assay for anti-inflammatory. Proc. Soc. Exp. Biol. Med. 11, 544 - 547.

18. Zhao X, Tang Z, Zhang H, Atianjoh FE, Zhao JY, Liang L, Wang W, Guan X, Kao SC, Tiwari V, Gao YJ, Hoffman PN, Cui H, Li M, Dong X, Tao YX. A long noncoding RNA contributes to neuropathic pain by silencing Kcna2 in primary afferent neurons. Nat Neurosci. 2013;16:1024–103.

19. Kumatia, EK, Zoiku, FK, Asase, A, Tung NH. 2024. In vitro and in silico anti-malarial activity and cytotoxicity of n-hexyl 1-O-rutinoside (a glycoside) isolated from Annickia polycarpa (DC.) Setten and Maas ex I.M. Turner (Annonaceae). Journal of Ethnopharmacology 319 (2024) 117287.

20. Liu, Y., Yang, X., Gan, J., Chen, S., Xiao, Z.-X., Cao, Y., 2022. CB-Dock2: improved protein–ligand blind docking by integrating cavity detection, docking and homologous template fitting. Nucleic Acids Res. 50.

21. Willoughby, DA, DiRosa, M. 1972. Studies on the mode of action of non-steroid anti-inflammatory drugs. Ann Rheum Dis. 1972 Nov;31(6):540. doi: 10.1136/ard.31.6.540.

22. Crunkhorn, P, Meacock, SCR. 1971. Mediators of the inflammation induced in the rat paw by carrageenin. British Journal of Pharmacology. 42 (3); 392-402.

23. Morris, C.J. (2003). Carrageenan-Induced Paw Edema in the Rat and Mouse. In: Winyard, P.G., Willoughby, D.A. (eds) Inflammation Protocols. Methods in Molecular Biology, volume 225. Humana Press. https://doi.org/10.1385/1-59259-374-7:115.

24. Zhang, J.-M, An, J., 2007. Cytokines, Inflammation and Pain. Int Anesthesiol Clin. 2007; 45(2): 27–37.

25. Shavit Y, Fridel K, Beilin B – Postoperative pain management and proinflammatory cytokines: animal and human studies. J Neuroimmune Pharmacol. 2006; 1:443-451.

26. Foulkes, T, Wood, J. 2007. Mechanisms of cold pain. Channels, 1:3, 154-160, DOI: 10.4161/chan.4692

27. McDonald DI, Wood JN, Emery EC. 2020. Molecular mechanisms of cold pain. Neurobiology of Pain 7 (2020) 100044.

28. Kort, ME, Kym, PR. TRPV1 Antagonists. in Progress in Medicinal Chemistry, 2012.

29. Gilson, M.K., Given, J.A., Bush, B.L., McCammon, J.A., 1997. The statistical-thermodynamic basis for computation of binding affinities: a critical review. Biophys. J. 72 (3), 1047–1069.

30. Kumatia EK, Ayertey, F, Ohta T, Uto T, Tung NH. 2O23d. Iridoids from *Morinda lucida,* (Benth.) Rubiaceae, produced analgesic and anti-inflammatory activities via agonism at the kappa and delta opioid receptors, inhibition of COX-2 besides elevation of CAT and SOD activities. Journal of Ethnopharmacology 309 (2023) 116355. 1-12.

31. Zhou J, Wang B, Wang M, Zha Y, Lu S, Zhang F, Peng Y, Duan Y, Zhong D, Zhang S. 2024. Daucosterol alleviates heart failure with preserved ejection fraction through activating PPARα pathway. Heliyon 10 (2024) e38379.1-14.

32. Thanh, TB, Vu DL, Thanh HN, Tien VN, 2017. In vitro antioxidant and anti-inflammatory activities of isolated compounds of ethanol extract from Sanchezia speciosa Leonard's leaves, J Basic Clin Physiol Pharmacol [J] 28 (1) (2017) 79–84.

33. Jang J, Kim SM, Yee SM, Kim EM, Lee EH, Choi HR, Lee YS, Yang WK, Kim HY, Kim KH, Kang HS, Kim SH. 2019. Daucosterol suppresses dextran sulfate sodium (DSS)-induced colitis in mice, Int. Immunopharm. 72 (2019) 124–130.

34. Zhang F, Wang M, Zha Y, Zhou J, Han J, Zhang S, Daucosterol alleviates alcohol-induced hepatic injury and inflammation through P38/NF-kappaB/NLRP3 inflammasome pathway, Nutrients 15 (1) (2023).

Table

Table 1 is available in the Supplementary Files section.

Figures

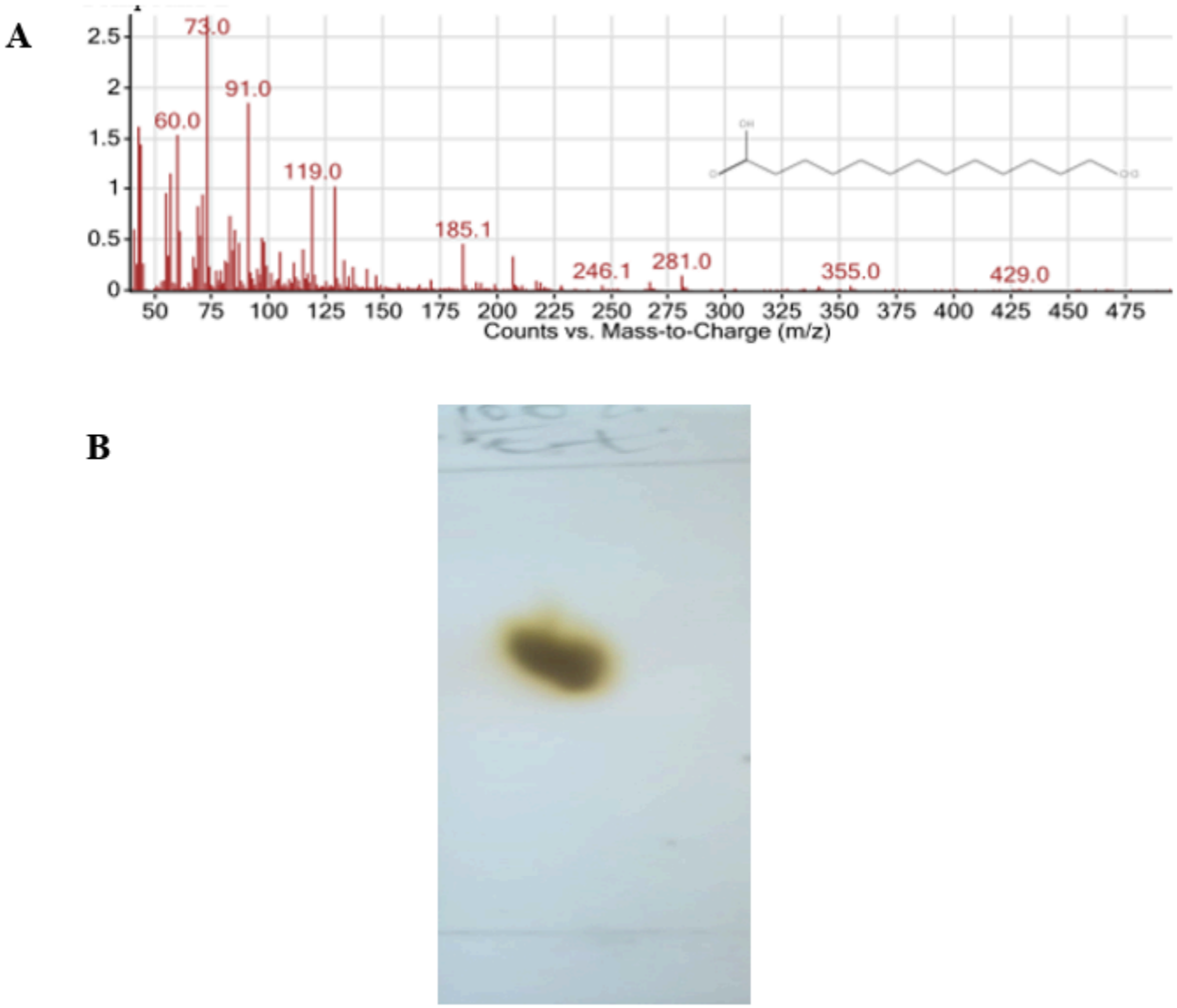

Figure 1

Structure of carboxylic acid derivative of [**1**] and its GC-MS spectrum retrieved from NIST database (A) and TLC chromatogram of [2], (B).

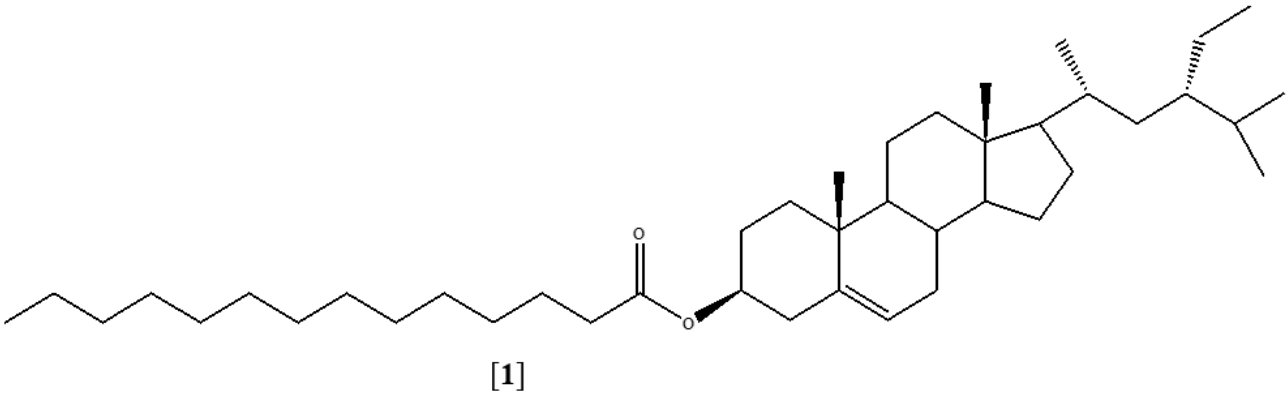

[**1**]

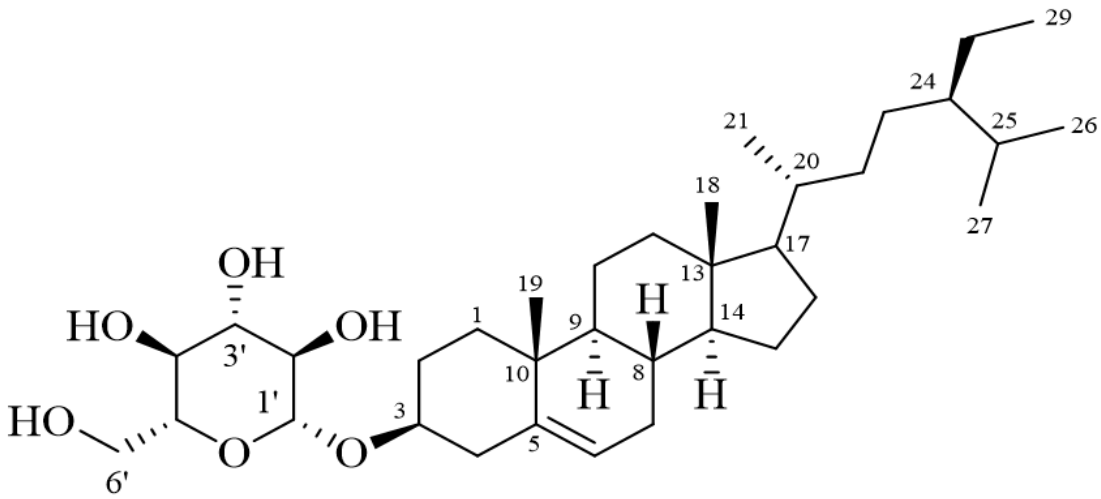

[2]

Figure 2

Chemical structures of *β*-sitosterol 3-myristate [**1**] and Daucosterol [**2**] isolated from *C. erythrocarpos* root bark.

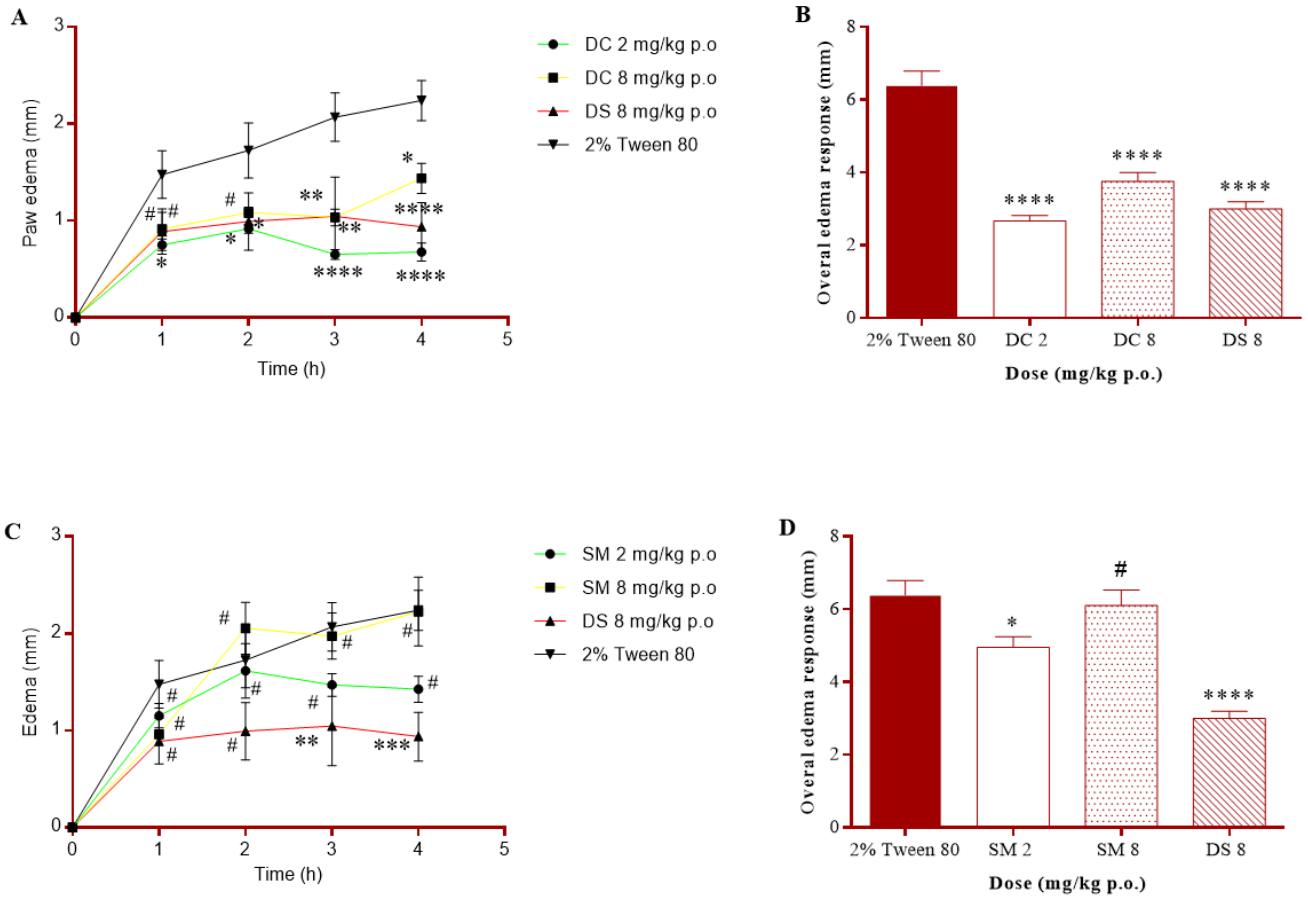

Figure 3

Effect of Daucosterol (DC), β-sitosterol 3-myristate (SM) and diclofenac sodium (DS) on carrageenan-induced edema in rats' paw on time cause curve (A) and (C) and overall edema response calculated as net area under the curve (B) and (D). *P < 0.05; **P < 0.01; ***P < 0.001 ****P < 0.0001 or #P > 0.05 compared to 2% Tween 80. Two-way ANOVA followed by Tukey's Post hoc test for the time course curve or one way ANOVA followed by Dunnett multiple comparison test for the overall edema response.

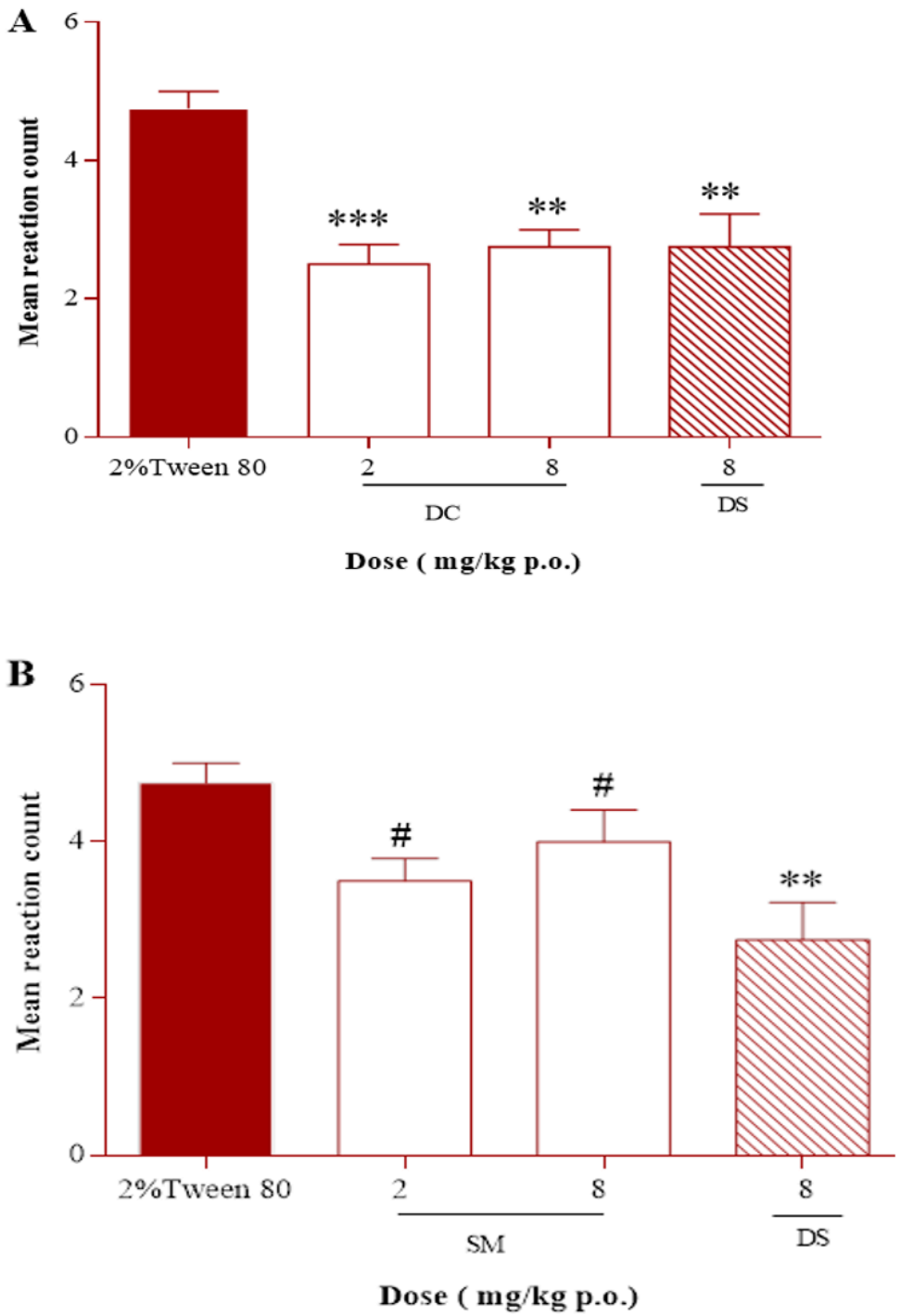

Figure 4

Effect of Daucosterol (DC), (A), β-sitosterol 3-myristate (SM), (B) and diclofenac sodium (DS) on mechanical hyperalgesia on rats' paw during carrageenan-induced inflammation on the fourth hour. *P < 0.05; *P < 0.01; *P < 0.001 or #P > 0.05 compared to 2% Tween 80 (One way ANOVA followed by Dunnett multiple comparison test).

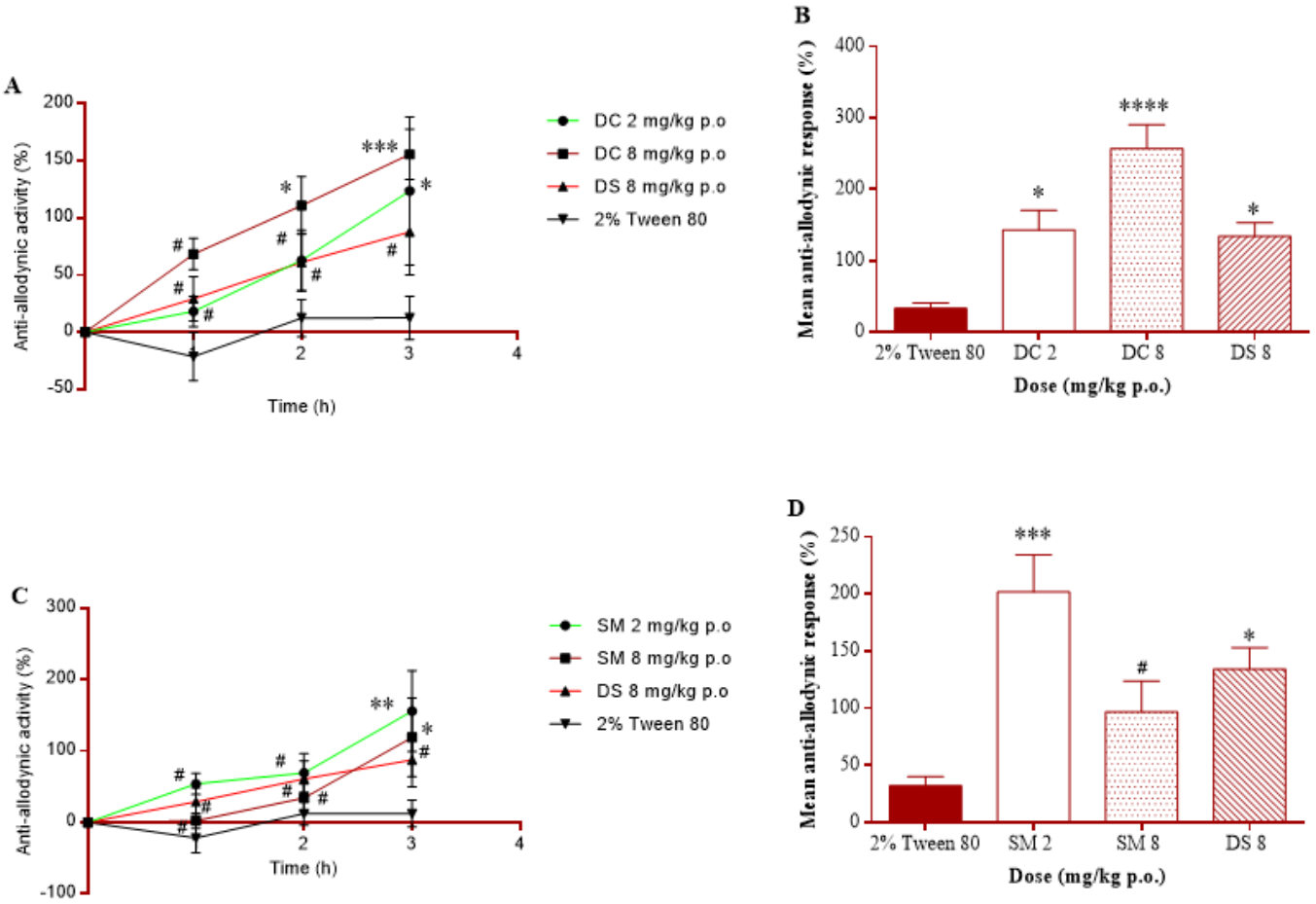

Figure 5

Effect of Daucosterol (DC), β-sitosterol 3-myristate (SM) and diclofenac sodium (DS) on cold-induced allodynia on rats' paw on time cause curve (A) and (C) and overall allodynic response calculated as net area under the curve (B) and (D). *P < 0.05; **P < 0.01; ***P < 0.001 or $^{\#}$P > 0.05 compared to 2% Tween 80. Two-way ANOVA followed by Tukey's Post hoc test for the time course curve or one way ANOVA followed by Dunnett multiple comparison test for the overall analgesic response.

Supplementary Files

This is a list of supplementary files associated with this preprint. Click to download.

- TABLE1.docx